Proceedings of the 2010 IEEE
International Conference on Mechatronics and Automation
August 4-7, 2010, Xi'an, China

Design and Optimization of Magnetic Wheel for Wall and Ceiling Climbing Robot

Yuanming Zhang, Tony Dodd, Kais Atallah, and Ian Lyne

Abstract—**Magnetic wall and ceiling climbing robots have been proposed in many industrial applications where robots must move over ferromagnetic material surfaces. The magnetic circuit design with magnetic attractive force calculation of permanent magnetic wheel plays an important role which significantly affects the system reliability, payload ability and power consumption of the robot. In this paper, a flexible wall and ceiling climbing robot with six permanent magnetic wheels is proposed to climb along the vertical wall and overhead ceiling of steel cargo containers as part of an illegal contraband inspection system. The permanent magnetic wheels are designed to apply to the wall and ceiling climbing robot, whilst finite element method is employed to estimate the permanent magnetic wheels with various wheel rims. The distributions of magnetic flux lines and magnetic attractive forces are compared on both plane and corner scenarios so that the robot can adaptively travel through the convex and concave surfaces of the cargo container. Optimisation of wheel rims is presented to achieve the equivalent magnetic adhesive forces along with the estimation of magnetic ring dimensions in the axial and radial directions. Finally, the practical issues correlated with the applications of the techniques are discussed and the conclusions are drawn with further improvement and prototyping.**

I. Introduction

THIS study aims to develop an autonomous mobile robot to enter a cargo container for the inspection of illegal contraband. In general, most standard cargo containers are made of corrugated ferromagnetic steel sheets built upon a steel frame structure. Whilst intended for carrying legal cargo these containers are often targeted for smuggling illegal contraband such as weapons, drugs, tobacco and humans. Border agencies spend considerable resources trying to detect such contraband. A potential solution is to send small robotic vehicles into cargo containers to search for the presence of contraband. Confined working spaces are targeted as various goods would take up most of the space inside the cargo container in most practical situations. In these cases, one possible solution is to design a magnetic wall and ceiling climbing robot (WCCR) to climb along the wall and ceiling of cargo container to implement the subsequent inspections. Furthermore, it is necessary to develop a light-weight and miniature volume of WCCR platform which can climb around the interior of the cargo containers with corresponding sensors and navigation system. Contraband detection is performed using trace detection sensors.

A great deal of research has been carried out to produce mobile robots with various functions for industrial inspection purposes, space exploration, urban search and rescue. In particular, magnetic climbing robots have attracted attention to address the problems of adhesive techniques and locomotion mechanism. For the ferromagnetic vertical wall and overhead ceiling of cargo containers, magnetic adhesion technique is considered as an effective approach to achieve an optimal solution rather than pneumatic vacuum sucker and other mechanical crawlers in practical applications.

So far, magnetic climbing robots have been proposed to apply to many industries [1]-[6], such as steel oil tank inspection, weld line inspection and steel pipe structure inspection. Moreover, various kinds of locomotion drive mechanisms have been explored by using magnetic wheels, magnetic tracks, magnetic grippers, magnetic feet and their integration.

It is noted that the magnetic circuit design with magnetic attractive force calculation of magnetic wheel significantly affects the system reliability, payload ability and power consumption of robots. As early as the 1990s, for example, Hirose and Tsutsumitake [1] proposed a pair of permanent magnet disks as magnetic wheels for design of wall climbing robot. FE method was proposed to calculate and estimate permanent magnet forces and magnet sizes for magnetic wheel robots. However, the magnetic circuit analysis was not presented, and the open-loop magnet disks with large size and heavy weight would be difficult to fulfill the light-weight requirement of the current WCCR. In recent years, the permanent magnetic track components were designed for the wall climbing robots, whereas permanent magnetic tracks were proposed to act as magnetic locomotion mechanism for oil tank and weld line inspections [2], [3], [4]. However, the magnetic tracked mechanisms might not be flexible to implement for the current corrugated shape wall and ceiling of cargo container. More recently, Tache *et al* [5], [6] described a magnetic motorbike robot with two magnetic wheels to climb and inspect ferromagnetic pipes with complex-shaped structures. However, the magnetic robot might be very complex to travel through vertical wall

Manuscript received March 16, 2010. This work was supported by UK EPSRC under Grant EP/G004307/1.

Tony Dodd and Yuanming Zhang are with the Department of Automatic Control and Systems Engineering, University of Sheffield, Sheffield, S1 3JD, UK (Tel: 0044-114-222-5636; Fax: 0044-114-222-5661; e-mail: t.j.dodd@sheffield.ac.uk, yuanming.zhang@sheffield.ac.uk)

Kais Atallah and Ian Lyne are with the Department of Electronic and Electrical Engineering, University of Sheffield, Sheffield, S1 3JD, UK (e-mail: k.atallah@sheffield.ac.uk, i.lyne@sheffield.ac.uk)

978-1-4244-5141-8/10/$26.00 © 2010 IEEE

to overhead ceiling of cargo container with the risk of falling down. Han *et al* [7] introduced a FE analysis to design a permanent magnet wheel to consider induction pins effective with magnetic full solid disks. However, some key issues were not involved to consider the current requirement of light-weight with hollow solid magnetic rings and optimization of wheel rims. In summary, the existing climbing robots would be difficult to satisfy the current requirements of cargo screening, especially as most of them have the characteristics of large size, heavy weight and rigid body.

In the present study, as magnetic wheeled climbing mechanisms with simple drive have advantages of high climbing speed and effective mobility compared with the tracked and legged locomotion, a flexible magnetic WCCR is proposed to be investigated in order to employ for cargo container screening process. To date, there has been little or no work done to develop a flexible WCCR with light-weight magnetic wheels and optimisation of wheel rims. Consequently, this paper aims to present a flexible robot with optimal design of magnetic wheels by using FE approach.

The paper is organized as follows. To begin with, a conceptual design of the flexible WCCR with six permanent magnetic wheels is presented to climb along the wall and ceiling of cargo container and a permanent magnetic wheel with a closed loop design is investigated. Next, FE approach is employed to estimate the permanent magnetic wheels with various wheel rims. Then the distributions of flux lines and magnetic attractive forces are compared for both in plane segment and corner section. An optimal wheel rim is presented to achieve the adhesive forces with the estimations of magnet dimensions in the axial and radial directions. Finally, following a discussion of the practical issues concerning the application of this technique, some conclusions are drawn together with further improvement and prototyping.

II. WCCR WITH MAGNETIC ADHESION

With reference to the cargo container screening process, it has some special requirements for design of WCCR, such as confined working space, convex and concave surfaces, and adhesion ability. Here, a flexible robotic platform is designed to climb along the wall and ceiling of a cargo container as shown in Fig. 1. As magnetic wheeled robots have good mobility and simple drive mechanism compared to magnetic tracked, legged or armed robots, six magnetic wheels are proposed for the use of the current WCCR. The front and back pairs of wheels are acted as driving wheels and the middle pair of wheels acted as following castors, whereas the flexible joint mechanisms are used to connect the three sections together to implement body bending motions (See Fig. 1a). The middle wheels support the payload section of the robot. Four universal joints are coupled to the drive wheels, and two spherical bearings are

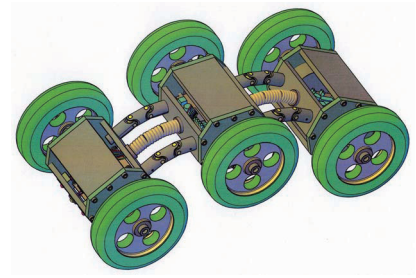

(a) Body bending

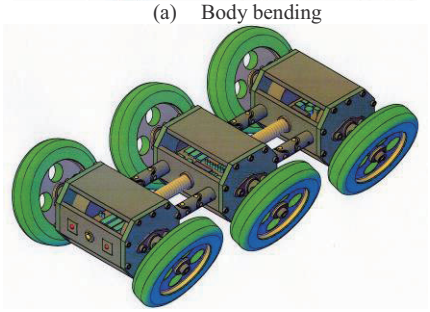

(b) Wheels bending

Fig. 1. Proposed robotic platform with flexible joints

used to fix the middle casters to achieve wheel bending motion (See Fig. 1b), so that WCCR has capability to adaptively work for the convex and concave surfaces of steel cargo container. The total weight of the current WCCR approximates 5.5kg including flexible mechanical body, stepper motors, magnetic wheels and electrical components with batteries, such as sensing, vision, navigating and driving system.

It is known that magnetic wheels are key components to produce enough adhesive forces for the current WCCR. There are several possible configurations to choose permanent magnets, such as rectangular magnetic block, magnetic disks, and magnetic segments. In this study, in order to produce a constant magnetic field, a preliminary design of magnetic wheel is showed in Fig. 2(a) and (b) with section view and 3D view, which comprises of a permanent

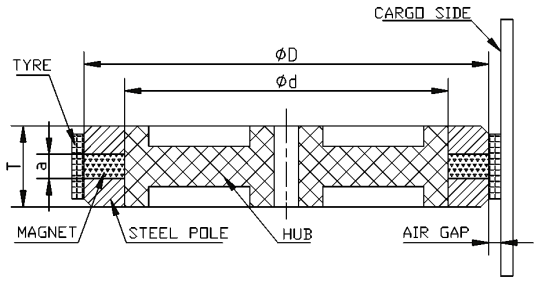

(a)Section view, ØD=96, Ød=76, T=20, and a=6 (mm)

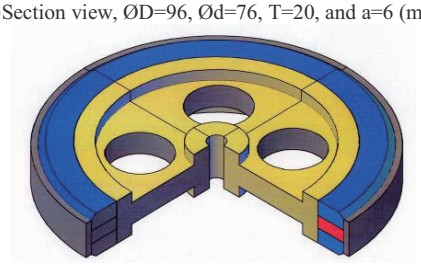

(b) 3D view

Fig. 2. Preliminary design of magnetic wheel with magnetic ring

magnetic ring with two side steel poles to adhere to central hub, and a simple rubber tire. Here, magnetic ring is magnetised through the axial thickness direction to constitute a closed-loop magnetic circuit with the steel poles, tire and contacted wall or ceiling area of cargo container, whereas the tire is acts as an air gap with various thickness to tune the attractive forces. Furthermore, for the current prototyping stage, the wheel tire is made by a thin rubber sheet with single and multilayer integration to choose a suitable tire thickness to achieve the corresponding magnetic attractive force as a variable air gap. The central hub is made of aluminum alloy material with four large holes to reduce the weight of wheel. As aluminum has low relative permeability (μ_r=1.0000037) [8], the central hub is approximately ignored as no-magnetic material in the magnetic circuit.

Considering the corrugated shape wall and ceiling of cargo container, four possible types of wheel edges were considered to adaptively climb both plane and V-type shape surfaces, as shown in Fig. 3 where *Sr* is relative to the special spherical radium, *Ta* is axial thickness, *Tw* is radial wall thickness of magnetic ring, respectively. During the initially phase, for magnetic ring, *Ta*=6mm and *Tw*=10mm, the axial thickness of steel pole is choose as 7mm. The four possible wheel edges are shown schematically in Fig. 3. (a) Square edge with minimum value *Sr*=0, (b) Fillet edge with small value *Sr*=2mm, (c) Chamfer edge with chamfer size of 2mm×2mm×45°, and (d) Sphere shape with maximum *Sr*=7mm. With reference to the variable edge configurations calculation of the magnetic forces and optimization of rims will be investigated in the next section.

III. Magnetic Wheel Design

As mentioned above, FE method has been employed for the analysis of magnetic field. Compared with the conventional analytical method, FE method provides a rapid and graphical insight solution to estimate the behavior of the magnetic field, which involves the element type and attributes, meshing, material properties, real constants, boundary conditions and other features to model the physical system, such as magnetic flux density, magnetic force distributions, magnetic flux line, magnetic field strength, and air gap effect. The following sub-sections will present a brief visualization of design of magnetic wheel and optimisation of wheel rims.

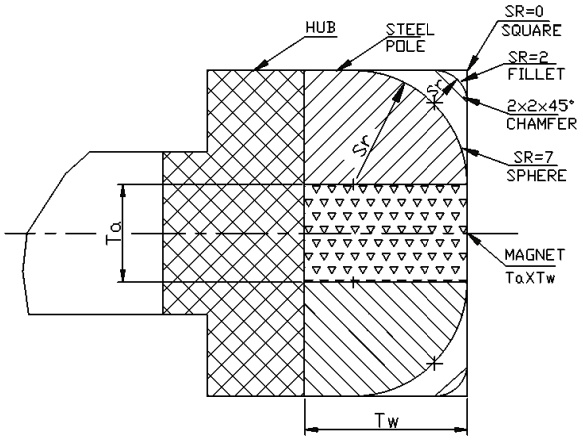

Fig. 3. Various rims shapes of magnetic wheel (a) Square edge (b) Fillet edge (c) Chamfer edge (d) Sphere shape

A. Magnetic Flux Lines and Forces

FE method for magnetic field analysis mainly involves procedures of geometry model building, element attribution, material proprieties, load apply with magnetic boundary and excitation, solution and results plot [9]. In general, there are two different methods to generate the geometry model. In this research, 2D geometry models (See Fig. 4) are produced by ANSYS direct generation and 3D geometry model (See Fig. 5) are created by AutoCAD importing SAT format to read into ANSYS.

It is also worthwhile to mention the definition of material properties of the magnetic wheel. For non-magnetic components, aluminum hub and rubber tire, the relative permeability are approximately set to be 1.0 as air medium. For magnetic unit, based upon the different chemical compositions of the carbon steels, steel poles and contacted steel cargo container, the relative permeability is approximately set to be 2000 and 1000 respectively [9].

In addition, it is critical to choose a suitable magnetic material for the permanent magnetic ring. Based upon magnetic compositions, typical commercialized magnets involve Neodymium Iron Boron (NdFeB), Samarium Cobalt (SmCo), Ceramic and Alnico [8]. It is known that NdFeB and SmCo are made from rare earth material, which can achieve excellent magnetic properties to create high magnetic forces compared with Ceramic and Alnico materials in the equivalent geometry conditions. Considering

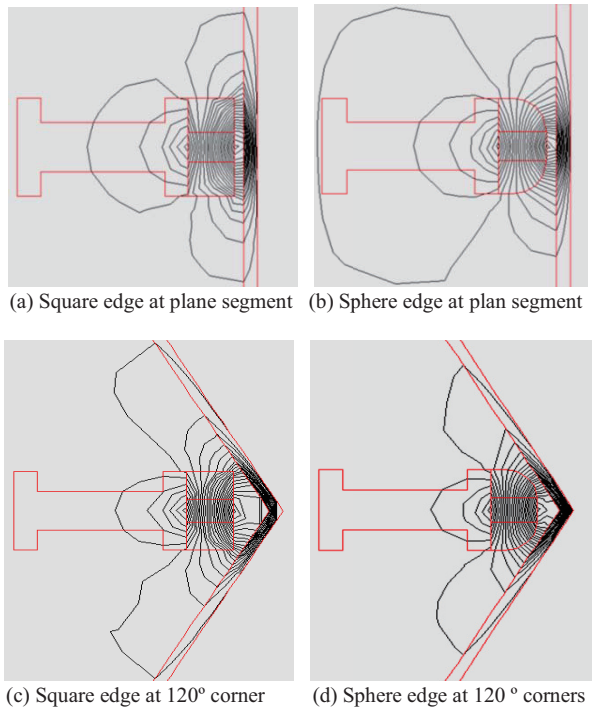

(a) Square edge at plane segment (b) Sphere edge at plan segment

(c) Square edge at 120º corner (d) Sphere edge at 120 º corners

Fig. 4. Distributions of magnetic flux lines

TABLE I
TYPICAL MAGNETIC CHARACTERISCS OF NdFeB N38

Properties	NdFeB N38
Remanence, *Br* (T)	1.23 to 1.30
Coercive force, *Hcb* (A/m)	≥860,000
Intrinsic coercive force, *Hcj* (A/m)	≥955,000
Maximum energy product, *BH* (KJ/m^3)	326 to 286
Temperature coefficient, *1/K*, *Tk* (HcJ)	-0.007
Max continuous temperature (°C)	80

the current applications to employ at room temperature with requirement of light-weight for WCCR, NdFeB is initially chosen to apply to the current design. For example, NdFeB serial N38 can work up to temperature 80°C and density around 7.45g/cm^3, it is cheaper and slightly lighter than the SmCo serial. Table I shows the typical magnetic characteristics of NdFeB N38 with main parameters, such as remanence magnetic density and coercive force.

Based upon the initial setting for FE analysis, it is known that permanent magnetic ring is acted as an excited component to apply loads with magnetic boundary. As mentioned earlier, the magnetic circuit mainly includes permanent magnetic ring, two side high permeability steel poles, tire as air gap, and contacted wall and ceiling of steel cargo container. The flux density and magnetic forces are calculated by using FE analysis. The typical results of magnetic flux lines distributions are shown in Fig. 4, with the square rim and spherical rim of wheel to climbing at the plane segment and V-type corner section, respectively. Here,

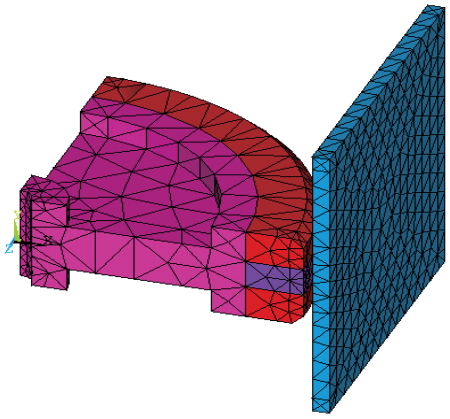

(a). Magnetic wheel modeling

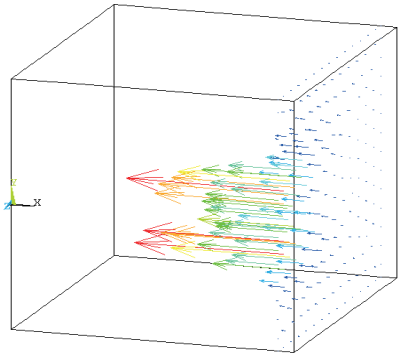

(b). Magnetic forces distribution

Fig. 5. Magnetic force analysis with 3D geometric mode (Quarter)

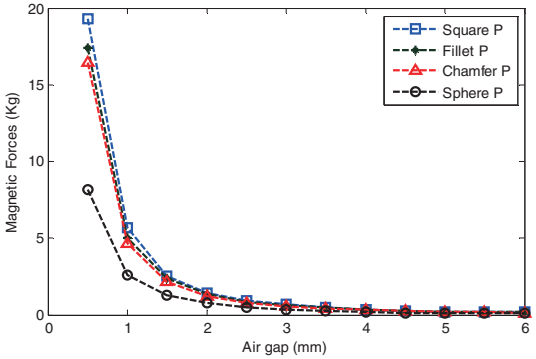

Fig. 6. Magnetic forces with various rims at plane segment

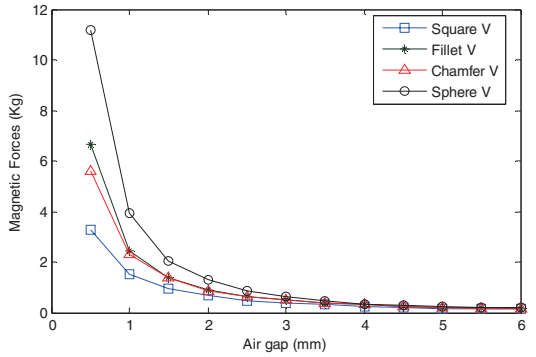

Fig. 7. Magnetic forces with various rims at 120º corner

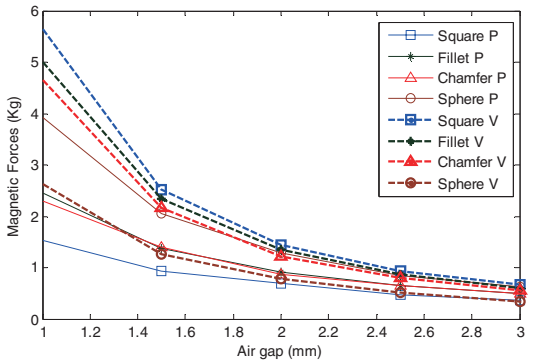

Fig. 8. Comparison of various magnetic forces

the thickness of wall and ceiling is set to be 3mm, and V-type angle is set equal to 120º as an indicative value for general cargo containers. It can clearly be seen that the square rims have good performances to work at the plane segment, on the contrary, the spherical rims have good performances to work at the corner condition.

In addition, the magnetic attractive forces exerted by a magnetic ring to the ferromagnetic cargo container can approximately be estimated by:

$$F_i = \lambda \times (B_i^{\,2} A_i) \tag{1}$$

$$F = \sum_{i=1}^{k} F_i \tag{2}$$

where F_i is the magnetic force, λ is the proportional coefficient, B_i is the magnetic flux density, A_i is the pole area, and F is the total magnetic attractive forces. However, regarding the B_i estimation, the wheeled geometry

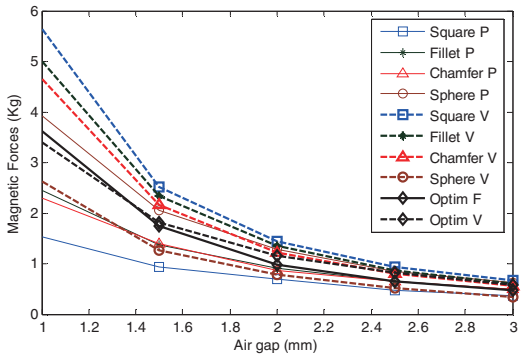

Fig. 9. Optimization of rims of magnetic wheel

dimensions have to be considered as the various air gaps, so that the magnetic holding forces might not be directly calculated by analytical method rather than a rectangular block with fixed air gap. However, in this scenario, FE method provides a rapid and effective solution for the current application. Although the magnetic wheel has symmetry structure along with an axis and centre, 2D FE model might not be suitable for the current magnetic force analysis.

Therefore, in this research, 3D FE model is explored as shown in Fig. 5(a), and the corresponding magnetic forces are shown in Fig. 5(b). The results indicate that the magnetic force varies with different air gap sizes and the maximum magnetic forces are created to form a symmetrical distribution in the contacted middle area, and magnetic forces rapidly reduce outside this area. The magnetic attraction results are showed in Fig. 6 and Fig. 7 with four types of wheel rims to climb at an ideal plane segment and V-type corner section, respectively, whereas magnetic ring is set to equal the outside diameter 96mm, inside diameter 76mm, and axial thickness 6mm. Compared with the two figures, a distinguished gap area of magnetic forces can be discovered between working at a plane segment and at a corner section. Moreover, that means an optimal design can be achieved by modifying the edge of poles.

B. *Optimization of Wheel Rims*

According to equations (1) and (2), the contacted magnetising area affects the magnetic forces along with magnetic flux density. As shown above, the surface areas of

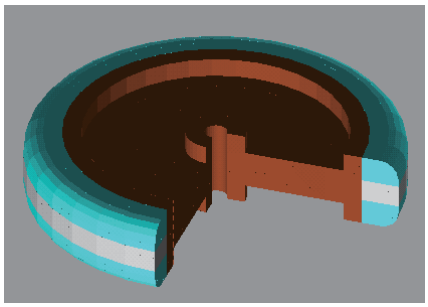

Fig. 10. Optimization of magnetic wheel

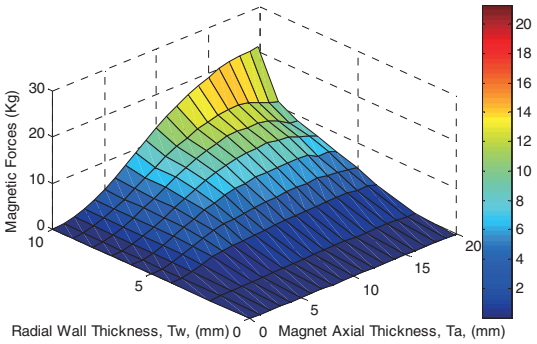

Fig. 11. Relationship of magnetic forces and magnet size

the wheel rims is varied from minimum *Sr*=0 to the maximum *Sr*=7mm, which alternately appear the opposite performances at plane segment and corner section. As an example, the thickness of rubber tire is chosen to work at thickness 1.5mm as shown in Fig. 8, it can be seen that there is a large variation of 1.8kg, from 2.8kg at plane segment to 1.0kg at corner section for *Sr*=0 case, whereas the variation is only 0.8kg, from 2.3kg to 1.5kg, for *Sr*=9mm case. Furthermore, the right angle rims have a good performance to work at plane surface, and have a poor performance to work at corner section, and vice-versa, for pure spherical rims. In addition to consider the motor characteristics of rotating speed and torque output, the equal magnetic forces are expected to achieve to implement for both plane and corner conditions. Therefore, an optimal design has been carried out as shown in Fig. 9. The optimal results show that the similar magnetic forces (1.8kg) have been achieved to work for both plane and corner circumstances, and optimisation of geometry model is shown in Fig. 10 with the spherical radium *Sr*=5mm.

C. *Estimation of Permanent Magnet*

With reference to wheel rim optimization procedure, the permanent magnetic ring was assumed to have fixed geometry dimensions in the axial and radial directions. However, the magnetic unit might have various choices to increase or decrease the magnetic ring dimensions to change axial thickness (*Ta*) or radial wall thickness (*Tw*). Considering the preliminary magnetic wheel is predetermined with diameter 96mm and thickness 20mm,

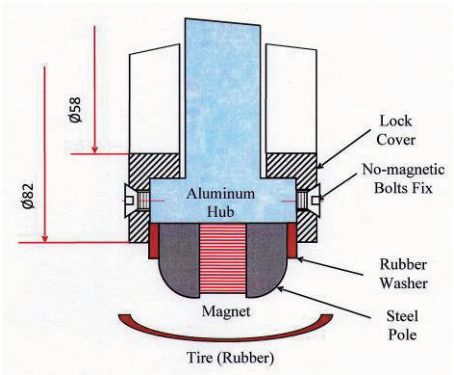

Fig. 12. Final optimization with collision prevention mechanism

the relationship of magnetic attractive forces *F* with magnetic axial thickness *Ta* and radial wall thickness *Tw* are shown in Fig. 11. It can be seen, regarding the axial thickness, for example, if *Ta* is set to be 8mm, magnetic attractive forces *F* gradually increases to maximum 120N with *Tw* increases to reach 15mm, and then *F* start to decrease even though magnet axial thickness still increases to maximum value 20mm. Furthermore, the simulation results show that the magnetic axial thickness significantly affects the magnetic forces in the closed-loop magnetic circuit. However, with the increase of magnet axial thickness, the steel pole thickness starts to reduce as well as the magnetic force until to work in the open-loop conditions.

In addition, regarding the radial wall thickness, for example, as *Ta* is set up to be 6mm, *F* rapidly increases to be 50N with *Tw* gradually reaching 6mm, and then *F* only slightly increases from 50N to 60N with *Tw* continuously changing from 6mm to maximum 10mm. In this case, the magnet radial thickness can be less than the steel poles (10mm), and magnetic attractive forces are only affected slightly. Furthermore, this configuration would reduce the possibility of a collision to directly strike the magnetic ring. Considering the robot total weight (5kg) in the preliminary design, *Ta* is initially chosen to set to be 6mm and *Tw* is chosen to set to be 9mm. The final magnetic forces would significantly be affected by tire thickness, and the initial tire thickness would be adjusted from 1.0mm to 5.0mm. In summary, the final optimal design is shown schematically in Fig. 12, which also adds a pair of rubber washers to reduce the impact of unforeseen collisions on the fragile magnet. In addition a pair of lock covers is added to prevent the axial movement of the magnetic unit.

IV. DISCUSSION

Some main issues are briefly discussed which are relative to FE method, magnetic wheel manufacturing and assembly, and magnet material properties. As mentioned earlier, FE method is an effective and powerful approach to predict magnetic forces for design of magnetic wheel, especially, for design of non-standard wheel. However, as the current FE method is an approximate estimation based upon certain assumptions, an experimental study is required to verify the current predictions.

In addition, to manufacture this type of magnetic ring it would be suggested to use magnetic segments or small size magnetic disks instead of the use of the whole ring to reduce the cost in this stage. However, this might result in an additional expense in the assembly stage, especially, for small magnetic disks. It would be difficult to produce an equilibrium magnetic field and stable magnetic forces causing an unstable locomotion. As additional metal bolts and pins would potentially affect the magnetic forces distributions, it would be suggested to use non-magnetic bolts or set to distant magnetic field induction.

On the other hand, FE method would also be useful in the design of light-weight aluminum hub and choosing a suitable rubber tire through further stress and strength analysis. For magnetic materials, at normal temperature, NdFeB magnets exhibit the good performance of all magnet materials. For example, NdFeB N38 is a good choice for the current wheel design. However, other high performance materials, such as NdFeB N52 would be outstanding to reduce the weight of magnetic wheel even more. Other practical issues, such as magnetic dust or particle removal, collision prevention, and magnetic leakage will also be investigated further after prototyping is built out.

V. CONCLUSIONS

In this study, FE method has been used for the design of magnetic wheels. This is a very effective approach to explore magnetic flux distributions and predict magnetic forces. A conceptual design of a flexible magnetic WCCR has been proposed to detect contraband within steel ferromagnetic cargo containers. Various wheel rims have been discussed to climb the corrugated shape cargo surface, and an optimal design has been carried out to alternately work at both condition of a plane segment and a V-type corner section with the equivalent adhesive forces. Permanent magnetic ring in the axial and radial directions has been estimated to explore the relationship of magnetic force. The prototype of magnetic wheel will be built and experimental study will be carried out to verify the current design in the next step.

ACKNOWLEDGMENT

The authors are grateful for the financial support of the UK EPSRC under grant reference EP/G004307/1.

REFERENCES

[1] S. Hirose and H. Tsutsumitake, "Disk Rover: A Wall-climbing Robot Using Permanent," in *Intelligent Robots and Systems, 1992, Proceedings of the 1992 IEEE/RSJ International Conference on*, 1992, pp. 2074-2079.

[2] Z. L. Xu and P. S. Ma, "A wall-climbing robot for labeling scale of oil tank's volume," *Robotica,* vol. 20, pp. 209-212, Mar-Apr 2002.

[3] J. Shang, B. Bridge, T. Sattar, S. Mondal, and A. Brenner, "Development of a climbing robot for inspection of long weld lines," *Industrial Robot,* vol. 35, pp. 217-223, 2008.

[4] W. Shen, J. Gu, and Y. Shen, "Permanent magnetic system design for the wall-climbing robot," Niagara Falls, ON, Canada, 2005, pp. 2078-2083.

[5] F. Tache, W. Fischer, R. Siegwart, R. Moser, and F. Mondada, "Compact magnetic wheeled robot with high mobility for inspecting complex shaped pipe structures," Piscataway, NJ 08855-1331, United States, 2007, pp. 261-266.

[6] F. Tache, W. Fischer, G. Caprari, R. Siegwart, R. Moser, and F. Mondada, "Magnebike: A Magnetic Wheeled Robot with High Mobility for Inspecting Complex-Shaped Structures," *Journal of Field Robotics,* vol. 26, pp. 453-476, 2009.

[7] S. C. Han, J. Kim, and H. C. Yi, "A novel design of permanent magnet wheel with induction pin for mobile robot," *International Journal of Precision Engineering and Manufacturing,* vol. 10, pp. 143-146, 2009.

[8] P. Campbell, *Permanent magnet materials and their applications*: Cambridge University Press, 1996.

[9] ANSYS Inc., *Electromagnetic field analysis guide*, 2002.